Supplementary Information

Synthesis and Sonication-Induced Assembly of Si-DDR Particles for Close-Packed Oriented Layers

Eunjoo Kim,[a,⊥] Wanxi Cai,[a,⊥] Hionsuck Baik,[b] Jaewook Nam,[c,*] and Jungkyu Choi[a,d,*]

[a] Department of Chemical and Biological Engineering, Korea University, Anam-dong, Seongbuk-gu, Seoul 136-713, Republic of Korea

[b] Korea Basic Science Institute, Seoul Center, Anam-dong, Seongbuk-gu, Seoul 136-713, Republic of Korea

[c] School of Chemical Engineering, Sungkyunkwan University, 2066 Seobu-ro, Jangan-gu, Suwon, Gyeonggi-do 440-746, Republic of Korea

[d] Green School, Korea University, Anam-dong, Seongbuk-gu, Seoul 136-713, Republic of Korea

[⊥] These two authors contributed equally to this work.

* Corresponding Authors

(JC) E-mail address: jungkyu_choi@korea.ac.kr, Phone: +82-2-3290-4854, and Fax: +82-2-926-6102

(JN) E-mail address: jaewooknam@skku.edu, Phone: +82-31-290-7349, and Fax: +82-31-290-7272

Experimental Procedure

S1. Preparation of α-Al_2O_3 discs

Porous α-Al_2O_3 discs were home-made by pressing α-Al_2O_3 powder (Baikowski CR 6 grade) into a disc (diameter: ~22 mm and thickness: ~2 mm), followed by sintering in a furnace (Pluskolab, model: CRF-M20-UP). For sintering, molded α-Al_2O_3 discs were heated to 800 °C with the ramp rate of 1 °C, maintained at 800 °C for 30 h, again heated to 1180 °C with the ramp rate of 1 °C, maintained at 1180 °C for 12 h, and cooled slowly down to room temperature. The average pore size of the α-Al_2O_3 disc thus obtained was ~ 170 nm with ~40% porosity. Further, one side of the α-Al_2O_3 disc was polished using a silicon carbide abrasive paper (Daesung, South Korea, CC-1500Cw).

S2. Synthesis of Si-DDR Zeolite Particles by Non-Seeded Growth

The experimental procedure based on the reported method in the literature[1] was conducted. 1-Adamantylamine (ADA 97%, Sigma-Aldrich) was first dissolved in ethylenediamine (EDA 99.5%, Sigma-Aldrich) in a capped plastic bottle by ~30 min sonication (JEIO TECH, UC-10P). After adding deionized water to the ADA and EDA mixture, it was homogeneously mixed using a shaker (Lab. Companion, SI-300R) for ~1 h. Subsequently, the resulting solution in the plastic bottle was refluxed at ~95 °C in a silicon oil bath for 3 h. Next, the silica source, tetramethyl orthosilicate (TMOS 99%, Sigma-Aldrich), was injected to the solution in the capped plastic bottle through a needled syringe, while the plastic bottle was still placed in the silicon oil bath (~95 °C). After additional reflux at ~95 °C for 3 h, the solution was transferred to a Teflon liner. The final molar composition of the synthesis solution was 47 ADA: 100 SiO_2: 404 EDA: 11,240 H_2O. The Teflon liner containing the reaction solution was sealed in an autoclave and rotated at ~40 rpm for ~25 d in an oven pre-heated to 160 °C. After the completion of the reaction, the autoclave was quenched in tap water. This synthesis protocol is referred to as TMOS-HT.

In addition to the high-temperature hydrolysis of TMOS (TMOS-HT), we adopted another approach (TMOS-Hd) for preparing the solution as follows: TMOS was hydrolyzed in deionized water overnight at room temperature. Subsequently, the ADA and EDA solution mixture was added to the pre-hydrolyzed TMOS solution. Finally, the synthesis solution was stirred at room temperature before transferring to the Teflon liner. The final molar composition was also 47 ADA: 100 SiO_2: 404 EDA: 11,240 H_2O. After this step, the same experimental procedure as used in TMOS-HT was carried out. The schematic summary delineating the protocol for synthesizing NSG-HT and NSG-Hd is provided in Scheme S1.

S3. Synthesis of Si-DDR Zeolite Particles by Seeded Growth

The Si-DDR particles obtained by the abovementioned non-seeded growth were used as seed particles for forming Si-DDR particles. The entire preparation procedure was identical to the non-seeded growth, except that we used a different silica source, namely CAB-O-SIL fumed silica (Cabot Corporation, M5 grade). A certain amount (10, 100, and 500 mg) of as-synthesized seed particles was added to the prepared synthesis solution (~30 g) kept in a Teflon liner. The corresponding weight percents of the seed crystals were 0.03, 0.33, and 1.6 %, respectively. The Teflon liner containing the reaction solution (final molar composition: 9 ADA: 100 SiO_2: 150 EDA: 4,000 H_2O as reported in the literature[2]) including seed particles was sealed in an autoclave and rotated at ~40 rpm in a preheated oven (160 °C) for ~4 d. After completion, the autoclave was quenched in tap water. The Si-DDR particles synthesized by seeded growth were calcined at 550 °C for 12 h. The schematic of the procedure adopted for seeded growth is illustrated in Scheme S2. In addition, seed particles (NSG-HT, ~0.1 g) were exposed to the synthesis solution used for seeded growth for 4 d, while the silica source of CAB-O-SIL was excluded from the solution.

S4. Sonication-Induced Assembly of Si-DDR Particles

For coating the Si-DDR particles, dried Si-DDR particles (~0.05 g) were first added to a glass reactor. Then, dried α-Al_2O_3 discs sandwiched by two cover glasses (Catalog No. 12-545-101, Fisher Scientific) were placed vertically on top of the Si-DDR particles using a Teflon holder. Anhydrous toluene (~40 mL, 99.8%, Sigma-Aldrich) was subsequently poured into the glass reactor through a needled syringe. These procedures were conducted in argon environment. Later, the glass reactor was sealed by parafilm, and placed in a sonicator water bath (JEIO TECH, UC-10P). The sealed glass reactor was sonicated for ~20 min. The resulting α-Al_2O_3 discs were calcined at 450 °C for 4 h. For convenience, this deposition protocol is referred to as the sonication-induced assembly method.

S5. Characterization

The shape of Si-DDR zeolite particles and the top-view morphology of Si-DDR zeolite layers were characterized by scanning electron microscopy (SEM, Hitachi S-4300). Prior to analysis, all the samples were Pt-coated by sputtering (Hitachi E-1030). The crystallinity of the synthesized Si-DDR particles and the out-of-plane orientation of Si-DDR zeolite layers were verified by X-ray diffraction (XRD, Rigaku Model D/Max-2500V/PC diffractometer, Japan) using Cu K_α radiation (40 kV, 100 mA, λ=0.154 nm). θ/2θ theta configuration was adopted. The simulated powder XRD pattern of Si-DDR zeolite was generated using the Mercury software (available from www.ccdc.cam.ac.uk). The corresponding crystallographic information file (CIF) for Si-DDR zeolites was downloaded from www.iza-online.org. CPO index was calculated by comparing (101) and $(2\bar{1}3)$ reflections between the DDR coated layer and the constituting DDR powder as follows: $\mathrm{CPO}_{(101)/(2\bar{1}3)} = \left[I_{(101)} / I_{(2\bar{1}3)}\Big|_L - I_{(101)} / I_{(2\bar{1}3)}\Big|_P \right] / \left(I_{(101)} / I_{(2\bar{1}3)}\Big|_P \right)$ where P and L denote the powder and layer, respectively. Transmission electron microscopy (TEM) image, high resolution (HR) TEM image,

and selected area electron diffraction (SAED) pattern of SG-HT-100, irradiated by 300 kV of accelerated electron beam, were obtained using Tecnai G2 F30 ST. The corresponding simulated SAED pattern was generated by the JEMS software (Java Electron Microscope Simulator, Ver. 3.8406U2012). The fast Fourier transform (FFT) result of the HR TEM image was acquired using the Gatan digital micrograph software.

For permeation measurements, the Wicke-Kallenbach mode was adopted with the total pressure at both the feed and permeate sides being ~1 atm. 50%/50% CO_2/N_2 mixture was fed to a DDR membrane and the permeate was further carried by helium and on-line analyzed by using a gas chromatograph (GC, YL6100GC, Young Lin Instrument (South Korea)). Specifically, ~100 $cc \cdot min^{-1}$ flow rates of CO_2 and N_2 were fed to the membrane, while the permeating CO_2/N_2 gases were carried by the helium flow rate (~200 $cc \cdot min^{-1}$) to the GC column.

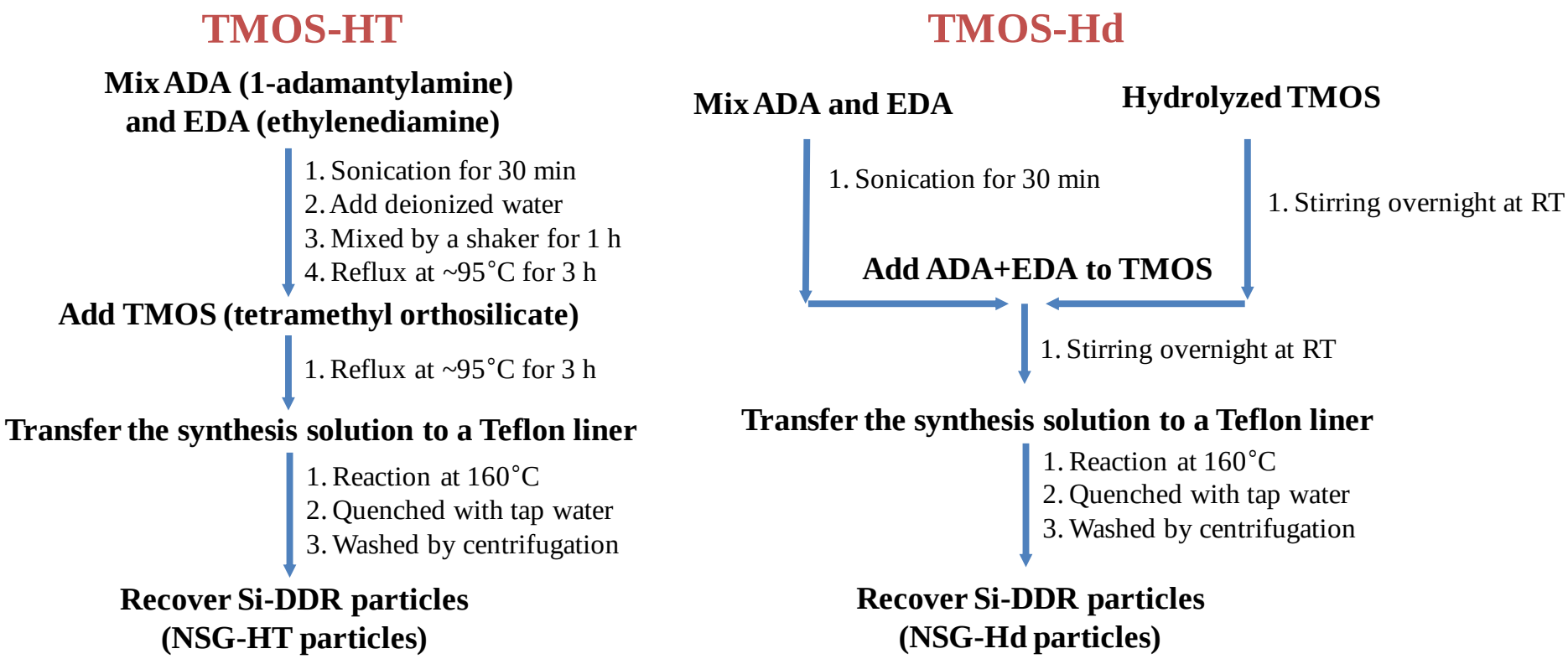

Scheme S1. Protocol adopted to synthesize Si-DDR zeolite particles (NSG-HT and NSG-Hd): TMOS HT (*left*) and TMOS Hd (*right*).

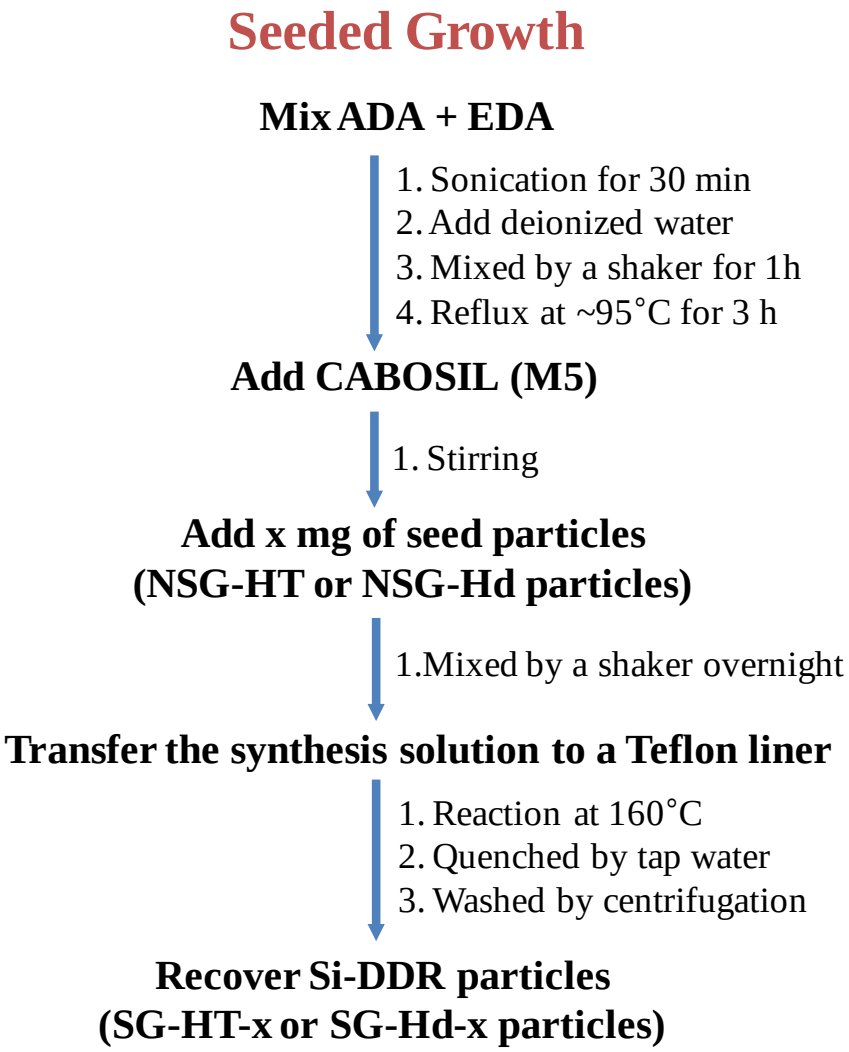

Scheme S2. Protocol to obtain Si-DDR particles (SG-HT-x and SG-Hd-x) via the seeded growth of NSG-HT and NSG-Hd, respectively.

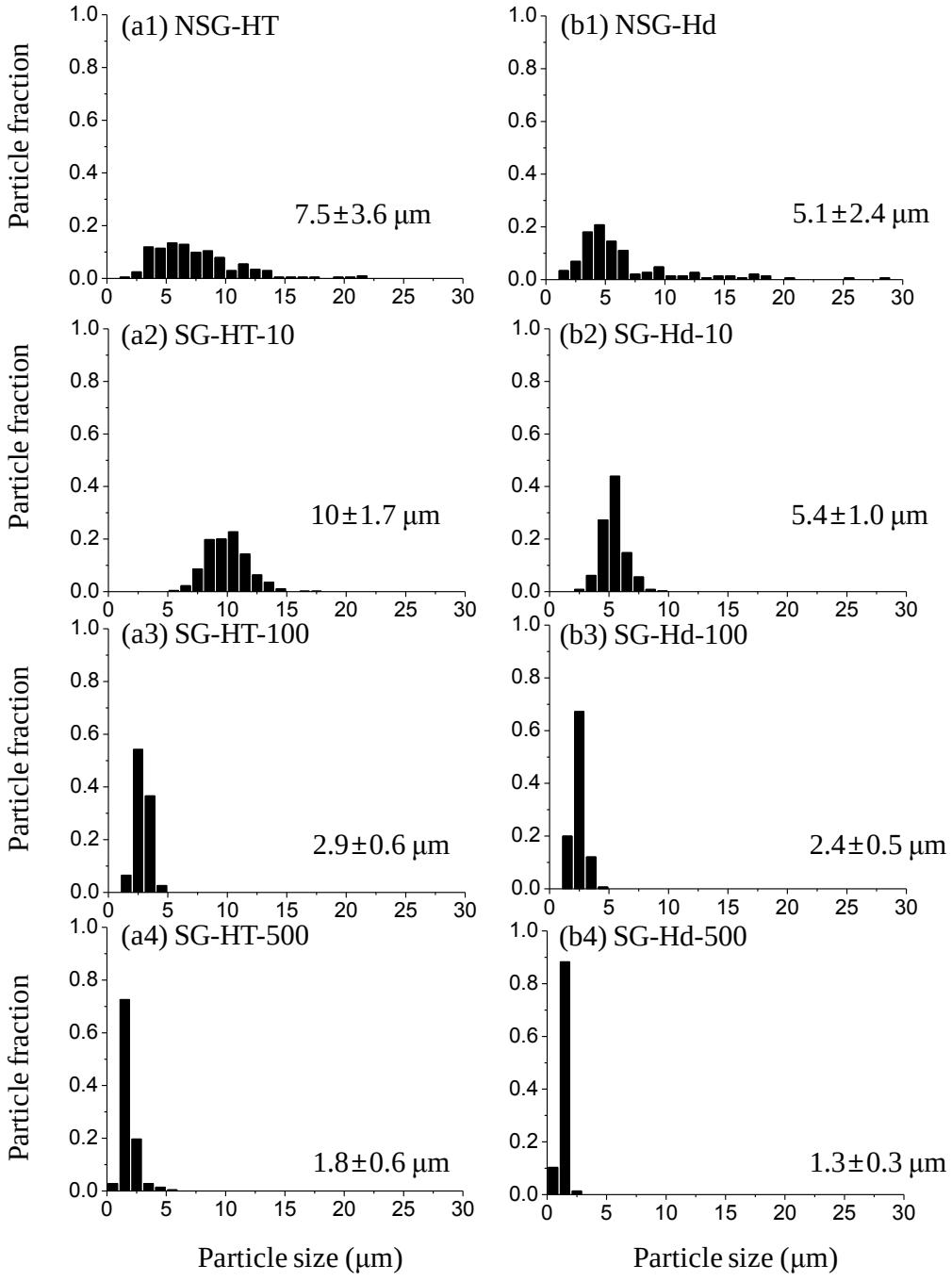

Figure S1. Particle size distribution of (a1)-(b1) particles obtained by the synthesis protocols of TMOS-HT and TMOS-Hd, respectively and particle size distribution of the particles synthesized in the presence of (a2)-(b2) 10 mg, (a3)-(b3) 100 mg, and (a4)-(b4) 500 mg of the particles shown in (a1)-(b1), respectively. Particle size was measured along the longest dimension. Average size and its standard deviation are displayed in each case.

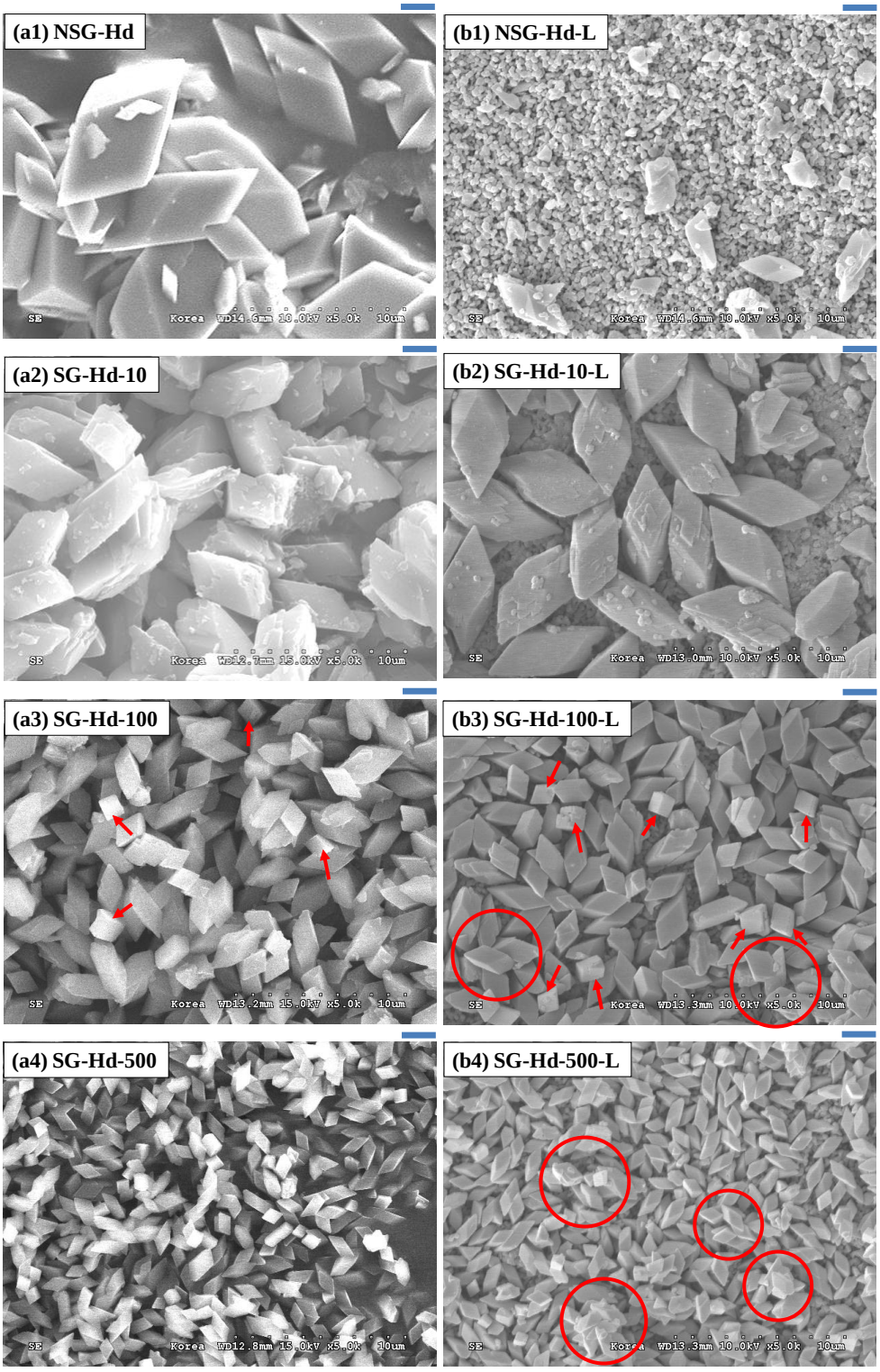

Figure S2. SEM image of (a1) particles obtained by TMOS-Hd synthesis protocol. SEM images of the particles synthesized by adding (a2) 10 mg, (a3) 100 mg, and (a4) 500 mg of particles shown in (a1) during seeded growth. (b1)-(b4) SEM images of layers NSG-Hd-L and SG-Hd-x-L (x=10, 100, and 500). In addition, non-diamond-like (e.g., cubic-like) particles are designated by red arrows in (a3) and (b3). Multilayered portions are marked in red circles in (b3) and (b4). The scale bars represent 2 μm.

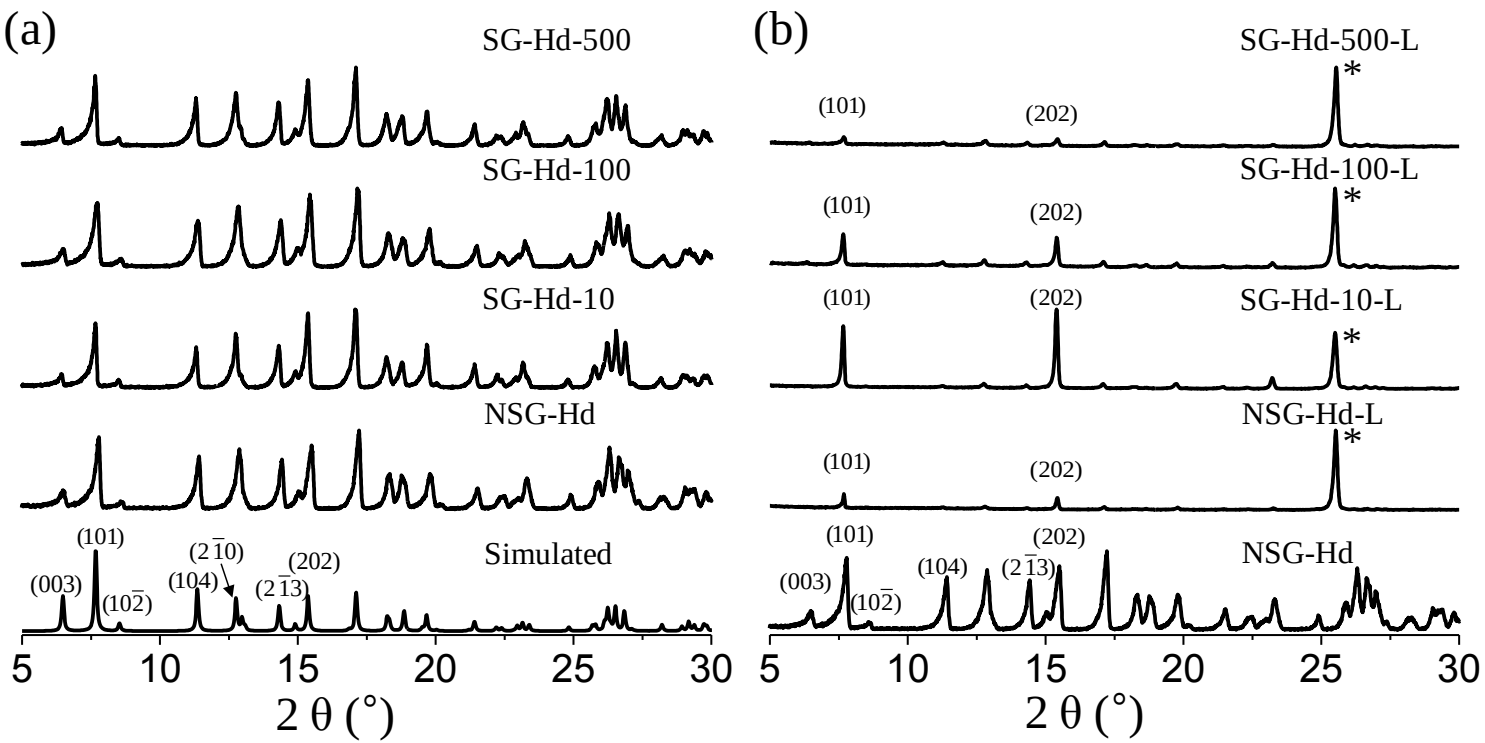

Figure S3. XRD patterns of (a) particles shown in Figure S2a1-a4 and (b) layers shown in Figure S2b1-b4. The simulated powder XRD pattern of Si-DDR zeolite is also included as a reference in (a). The XRD pattern of NSG-Hd is included for comparison in (b). Asterisk (*) in (b) denotes a peak from an α-Al_2O_3 disc.

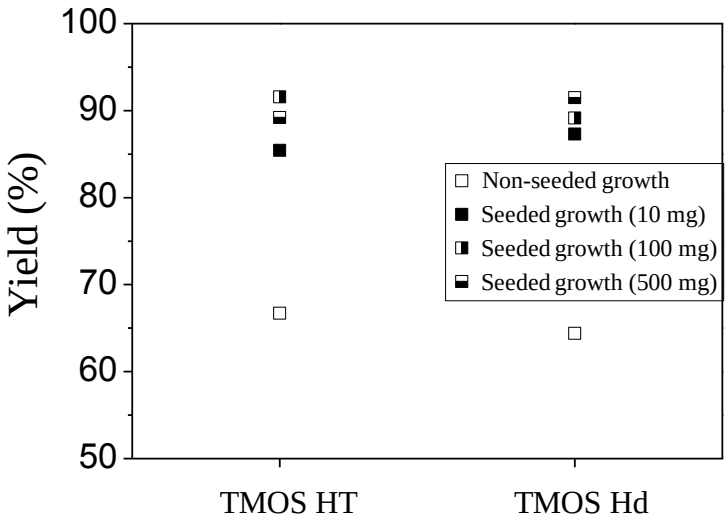

Figure S4. Yield of particles obtained by the synthesis protocols of TMOS-HT and TMOS-Hd, and particles obtained by the seeded growth of NSG-HT and NSG-Hd. For convenience, TMOS-HT and TMOS-Hd were used to designate particles (NSG-HT and NSG-Hd, respectively) obtained by the non-seeded growth and particles (SG-HT and SG-Hd, respectively) obtained by the seeded growth.

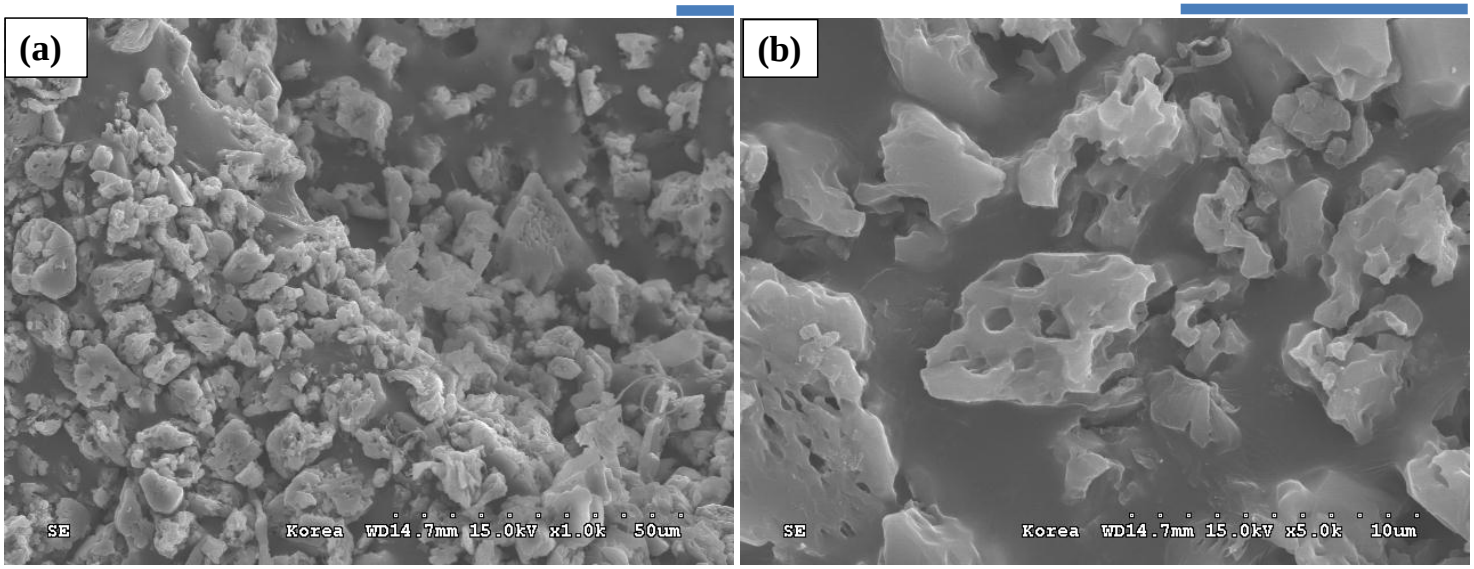

Figure S5. (a) Low magnification and (b) high magnification SEM images of particles obtained by exposing NSG-HT to the synthesis solution used for seeded growth for ~4 d, while the silica source (CAB-O-SIL) was not included. The scale bars represent 10 μm.

We adopted the synthesis solution (used for the seeded growth as described in S3) for secondary growth in an attempt to obtain continuous Si-DDR membranes. We conducted the secondary growth of SG-Hd-500-L layers at the 3 different reaction times (2 d, 4 d, and 6 d) to estimate the appropriate secondary growth time required for forming continuous membranes. In particular, SG-Hd-500-L layers which were comprised of the smallest DDR particles as compared to the SG-Hd-10-L and SG-Hd-100-L layers, were first chosen mainly because smaller particles allowed the less empty space between deposited particles in the seed layer, as reflected by the higher surface coverage in Fig. 4b. Fig. S6 reveals that continuous DDR films could be obtained by using the 2-6 d secondary growth and their surface morphology and random orientation were comparable to that of randomly oriented DDR membranes reported in the literature.[2-5] The secondary growth of the SG-Hd-500-L layer led to the formation of a randomly oriented film whose XRD pattern was almost identical to that of the DDR powder. The corresponding CO_2/N_2 permeation data through a membrane grown from SG-Hd-500-L via the 4 d secondary growth are shown in Fig. S7. The poor CO_2/N_2 separation performance can be attributed to the presence of apparent cracks observed throughout the membrane surface as indicated by red arrows in Fig. S6. Since it appears that 2 d for secondary growth was sufficient to achieve the inter-growth of deposited DDR particles as shown in Fig. S6a, we considered the synthesis times of 1 d and 2 d for the secondary growth of all seed layers (i.e., SG-Hd-10-L, SG-Hd-100-L, and SG-Hd-500-L layers).

It appears that a film grown from the SG-Hd-500-L layer was randomly oriented as compared to the DDR powder. The preferred *h0h*-orientation, observed in the SG-Hd-100-L layer (Fig. S3b), was not well preserved with the increased time, apparently because of the preferential growth along the longest dimension in the diamond-like shape toward the bulk solution, as addressed previously in MFI zeolite film growth.[6] In contrast, a membrane grown from the SG-Hd-10-L possessed a preferential *h0h*-out-of-plane orientation mainly due to the predominated out-of-plane orientation in the starting seed layer. Despite the observed continuity in all membranes under the SEM resolution, their CO_2/N_2 permeation data (maximum CO_2/N_2 separation factor of ~1.3) revealed that desired inter-growth of the grains in the

final DDR membrane was not achieved yet. This poor performance indicates that substantial, elaborate efforts to control secondary growth conditions are required for synthesis of oriented DDR membranes that show high CO_2/N_2 separation performance.

Specifically, Figs. S8 and S9 show the SEM images, XRD patterns, and CO_2/N_2 permeation data of the membranes grown from the SG-Hd-10-L, SG-Hd-100-L, and SG-Hd-500-L layers via the 1 d and 2 d secondary growth, respectively. It appears that the continuous DDR membranes were obtained by both 1 d and 2 d secondary growth for all seed layers. From the SG-Hd-500-L layer, its resulting membrane was randomly oriented, as the corresponding XRD pattern was similar to that of DDR zeolite powder. The degree of the out-of-plane orientation of the membrane, grown from the SG-Hd-100-L, was monotonically decreased with the increased secondary growth time: The corresponding CPO values after 1 d and 2 d secondary growth were ~3.6 and ~1.2, respectively, while the CPO value of the seed layer was ~4.1. The reduction of the out-of-plane orientation can be explained by the preferred growth of the longest dimension in the diamond-like DDR particles toward the bulk solution that fails epitaxial growth as previously addressed in the study of MFI zeolite film growth.[6] However, the SG-Hd-10-L layer, which was highly *h0h*-oriented, contributed to achieving the preferred *h0h*-out-of-plane orientation after secondary growth despite the above-mentioned undesired growth on the deposited seed particles: The corresponding CPO value (~25) was comparable to that of the seed layer (~20). It is worth mentioning that continuous, highly *h0h*-oriented DDR membranes could be obtained especially by carrying out the secondary growth of SG-Hd-10-L layers. However, the loss of the preferred out-of-plane orientation is expected to be pronounced with the elongated secondary growth time due to the above-mentioned undesired growth toward the bulk solution and accordingly, the failure of epitaxial growth.

Despite the continuous membranes observed by the SEM images in Figs. S8 and S9, the CO_2/N_2 permeation data indicated that the inter-growth between the DDR grains in the final membrane was not highly achieved yet, as reflected by the maximum CO_2/N_2 separation factor (SF) of ~1.3 (vs. ~0.8 SF

through α-Al_2O_3 discs due to the dominated Knudsen diffusion). Considering the fact that the previously reported randomly oriented DDR membranes showed ~20 CO_2/N_2 ideal selectivity[2, 3] and ~5 CO_2/N_2 ideal selectivity,[4] the DDR membranes obtained in this study were not inter-grown for realizing the intrinsic CO_2/N_2 separation ability of DDR zeolites. This poor CO_2/N_2 separation performance, in turn, indicates the importance of an appropriate secondary growth condition that allows less-defects in the final membranes. Currently, we are endeavoring to find proper secondary growth conditions that lead to the fabrication of continuous, *h0h*-oriented DDR membranes via the epitaxial growth of *h0h*-oriented DDR layers, especially SG-Hd-100-L and SG-HT-100-L layers as suggested by this study.

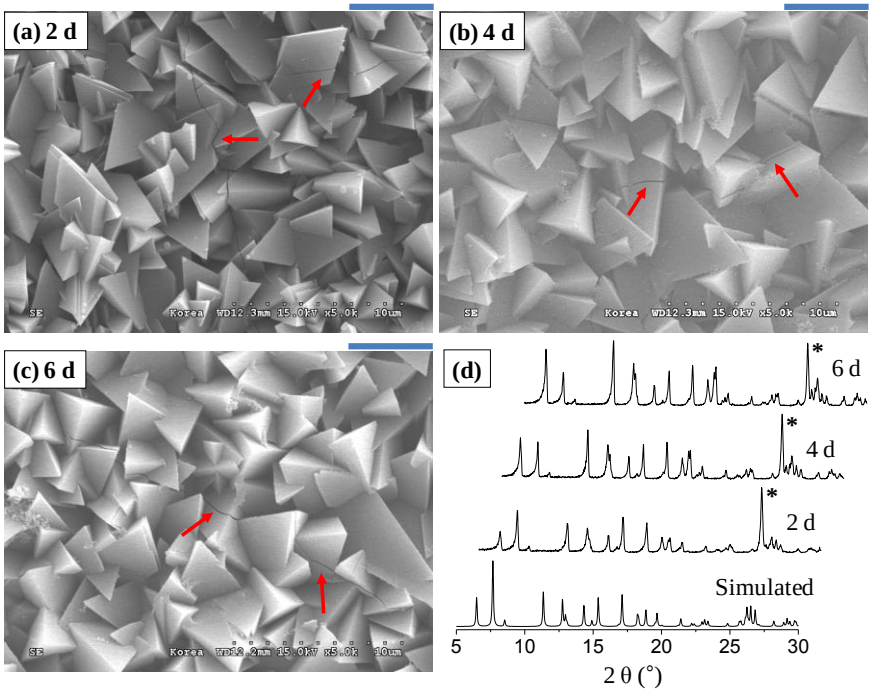

Figure S6. SEM images of calcined films obtained from the (a) 2 d, (b) 4 d, and (c) 6 d secondary growth of the SG-Hd-500-L layers and (d) the corresponding XRD patterns along with the simulated powder XRD pattern of DDR zeolites. The synthesis solution used for the seeded growth (described in S3) was also employed for manufacturing membranes. Cracks observed in the SEM images in (a)-(c) are indicated by red arrows and the scale bars represent 5 μm.

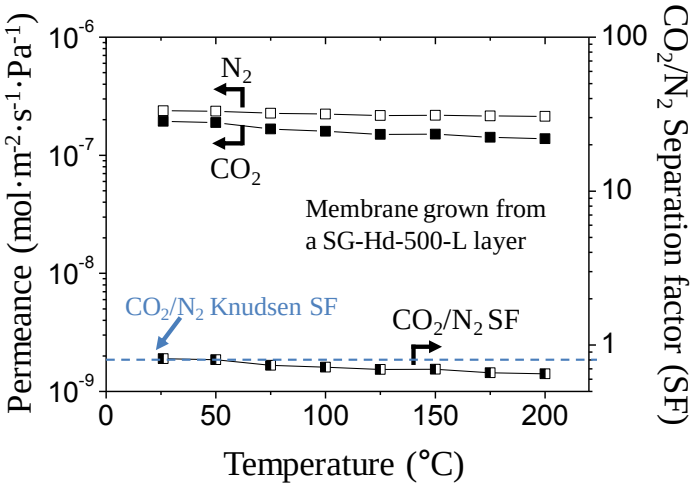

Figure S7. Permeances of CO_2 and N_2 through a membrane shown in Fig. S6b (i.e., grown via the 4 d secondary growth of a SG-Hd-500-L layer) and the corresponding CO_2/N_2 separation factor as a function of temperature. The ~0.8 ideal CO_2/N_2 separation factor (SF) under the Knudsen diffusion regime is denoted by the blue dashed line for comparison.

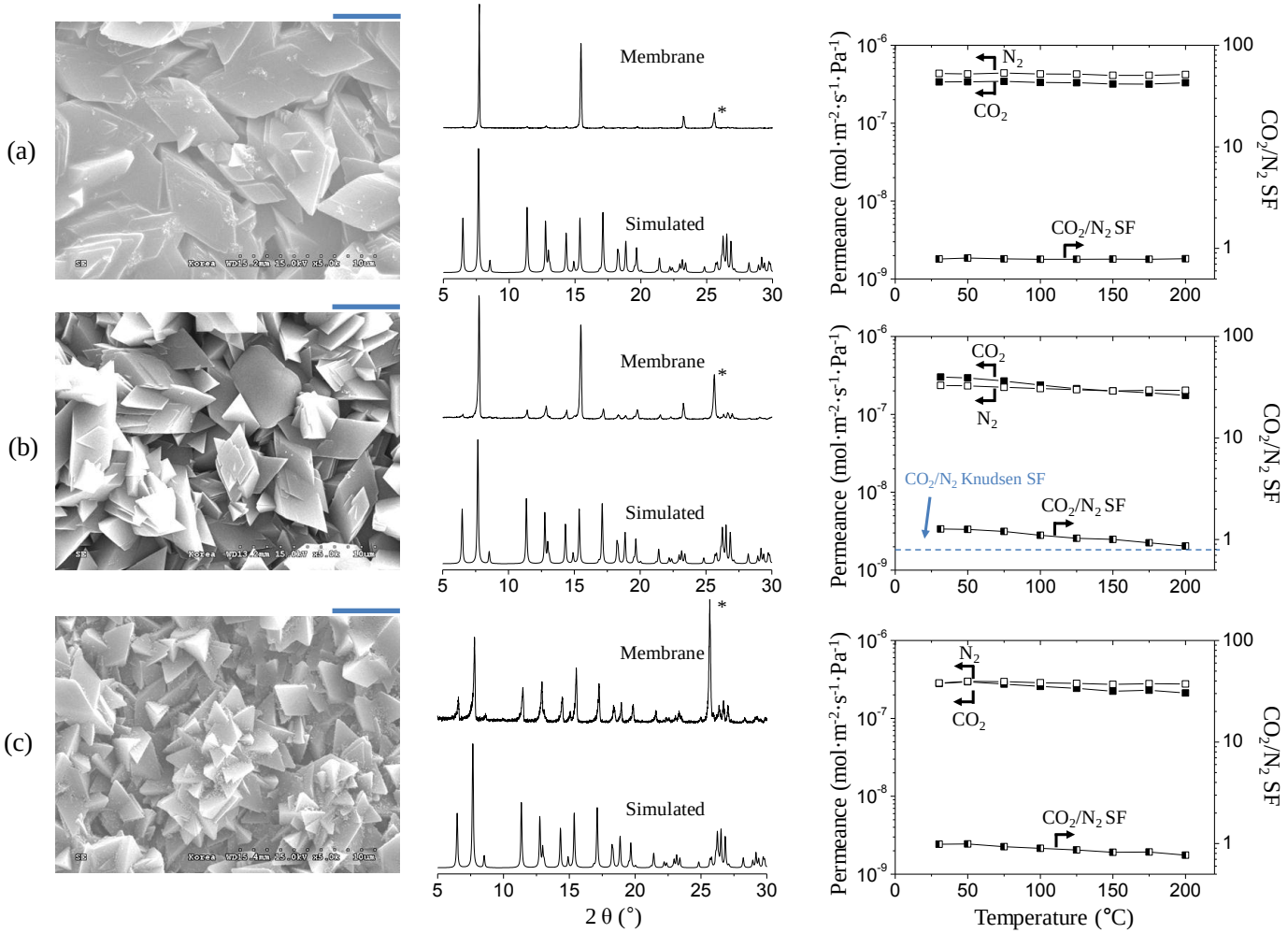

Figure S8. SEM image (*left*), XRD pattern (*middle*), and CO_2/N_2 permeation data (*right*) of DDR zeolite membranes, grown via the 1 d secondary growth of the (a) SG-Hd-10-L, (b) SG-Hd-100-L, and (c) SG-Hd-500-L layers. The scales bars above the SEM images represent 5 μm. In the XRD patterns, the simulated powder XRD pattern of DDR zeolite is also included for comparison and * denotes a XRD peak from an α-Al_2O_3 disc. In the CO_2/N_2 permeation data, CO_2/N_2 permeances and their SF are plotted against the temperature.

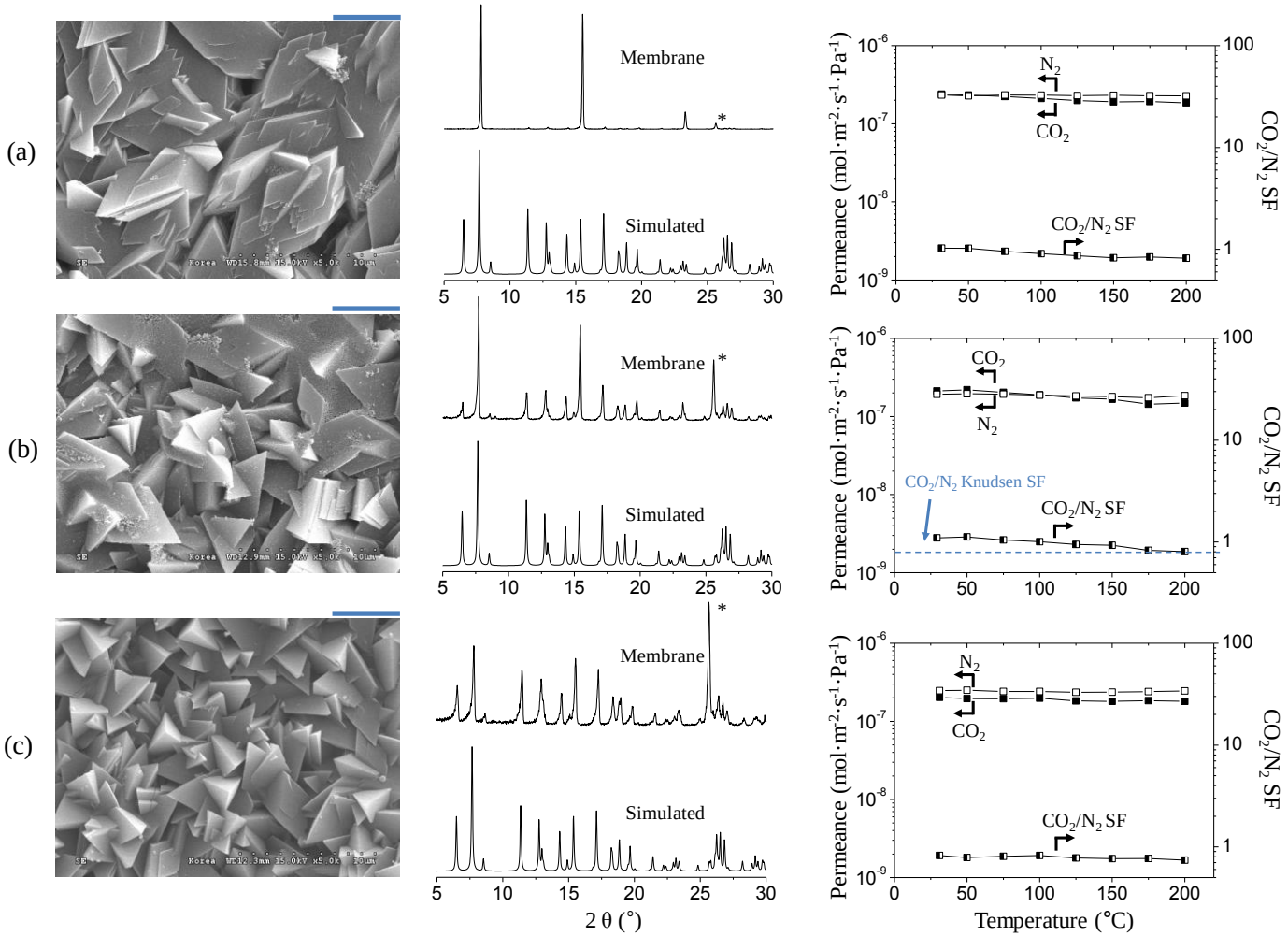

Figure S9. SEM image (*left*), XRD pattern (*middle*), and CO_2/N_2 permeation data (*right*) of DDR zeolite membranes, grown via the 2 d secondary growth of the (a) SG-Hd-10-L, (b) SG-Hd-100-L, and (c) SG-Hd-500-L layers. The scales bars above the SEM images represent 5 μm. In the XRD patterns, the simulated powder XRD pattern of DDR zeolite is also included for comparison and * denotes a XRD peak from an α-Al_2O_3 disc. In the CO_2/N_2 permeation data, CO_2/N_2 permeances and their SF are plotted against the temperature.

References

1. M.J. den Exter, J.C. Jansen, H. van Bekkum, *Stud. Surf. Sci. Catal.* 1994, **84**, 1159-1166.
2. T. Tomita, K. Nakayama, H. Sakai, *Micropor. Mesopor. Mater.* 2004, **68**, 71-75.
3. S. Himeno, T. Tomita, K. Suzuki, K. Nakayama, K. Yajima, S. Yoshida, *Ind. Eng. Chem. Res.* 2007, **46**, 6989-6997.
4. Z. Zhou, S. Nair, (Georgia Tech Research Corportation), US 2013/0064747 A1, **2013**.
5. M. Kanezashi, J. O'Brien-Abraham, Y.S. Lin, K. Suzuki, *Aiche J.* 2008, **54**, 1478-1486.
6. Z. Lai, G. Bonilla, I. Diaz, J.G. Nery, K. Sujaoti, M.A. Amat, E. Kokkoli, O. Terasaki, R.W. Thompson, M. Tsapatsis, D.G. Vlachos, *Science* 2003, **300**, 456-460.